Computer Simulation of Plasma Electron Collection by PIX-II

M.J. Mandell,* I. Katz,† and G.A. Jongeward*
S-Cubed, La Jolla, California
and
J.C. Roche‡
NASA Lewis Research Center, Cleveland, Ohio

An improved version of the NASCAP/LEO code has been used to model current collection by a positively biased solar array, as measured by the PIX-II flight experiment. The improvements consisted primarily of incorporation of a wake model and development of a solar array surface model. With these improvements, NASCAP/LEO predictions are in good qualitative agreement with the flight measurements. At both high and low bias, the predicted currents agree with experiment to within the uncertainties in the environment. Floating potentials and wake effects can also be calculated. Solar array snapover is predicted to occur at about 100 V. This is in reasonable agreement with laboratory observations, but agrees less well with the flight measurements, where snapover voltages tended to be somewhat higher.

Nomenclature

a = half-width of interconnect
A_n = Fourier coefficient of periodic surface potential
b = actual half-width of interconnect
E_I = first crossover energy for secondary electron emission
$E_z(x,y,z)$ = electric field normal to solar array surface
E_0 = mean normal electric field at solar array surface
$f(z)$ = normalized function describing the falloff of mean [averaged over (x,y)] potential with distance from the solar array surface
L = half-width of coverslip
x_M = variable describing position on coverslip where potential drops to E_I
$V(x,y,z)$ = electrostatic potential in space above solar array surface
$\bar{V}$ = mean potential of solar array surface
V_B = actual potential at center of coverslip
V_I = actual interconnect potential
V_0 = potential difference between interconnect and coverslip
z = distance from solar array surface
β = effective fractional area of interconnet
γ = function of interconnect fraction relating the electric field at the coverslip center to the potential difference between interconnect and coverslip
Δx = distance describing relation between mean surface potential and mean normal electric field
ξ = variable used to calculate x_M

Introduction

NASA Lewis Research Center has flown two Plasma Interaction Experiments, PIX-I[1] and PIX-II,[2] to study current collection by surfaces of high-voltage solar arrays in the space plasma environment. PIX-I included a bare metal disk and a disk-on-kapton experiment, as well as a 100-cm^2 simulated solar panel. PIX-II had a 2000-cm^2 solar panel, a Langmuir probe for plasma diagnostics, and an electron emitter. For both experiments, extensive measurements were made under laboratory plasma conditions prior to flight on a Delta second stage. PIX-I flew on March 5, 1978, in a 920-km polar orbit. PIX-II flew on January 25, 1983 at an altitude of approximately 900 km.

The two disk experiments aboard PIX-I were analyzed extensively by ourselves[3] and others.[4] Success in predicting the current to the plain disk showed the adequacy of our ideas about electrostatic potentials, currents, and sheath formation in plasmas when all surface potentials are known. The disk-on-kapton experiment proved far more interesting. Under positive bias conditions, the presence of an insulator suppressed current collection at low bias voltage ($\lesssim$100 V) and enhanced electron collection at high voltage (300 V). This effect was also studied in detail by Gabriel et al.[5,6] This "snapover" effect was recognized as a secondary electron phenomenon, and eventually both our group[3] (using an electric field boundary condition) and others[4] (using explicit transport of secondary electrons) were able to attain satisfactory agreement between calculation and experiment.

Roche[7] developed a NASCAP/LEO model for the PIX-II experiment. The model is similar to that shown in Fig. 1. The rocket body was resolved to 0.25 m. Through use of the local subdivision capability, the solar panel was resolved to 0.028 m. The solar cell areas were modeled as pure insulators, with the interconnects grouped together in two cells in each of the four segments. Calculations using this model, and comparison with the flight data, showed that the practice of lumped interconnects was not an adequate model of a solar array surface. In addition, the PIX-II experiment showed large fluctuations in the collected current for biases 100 V and lower. This is attributed to a slow tumbling of the Delta, which changed the orientation of the PIX experiment with respect to the velocity vector of the Delta. At low biases, where the electron sheath is close to the surface of the experiment, the shadowing of the ram ions by the spacecraft will produce a strong orientation dependence of the current collection. To be able to calculate this orientation dependence, a wake model was needed. Consequently, we proceeded to develop such models for NASCAP/LEO.

Solar Array Surface Model

Typical length scales involved in modeling a solar power system are: spacecraft size, 5.0 m; code resolution, 0.2 m; solar cell size, 0.02 m; interconnect size, 0.001 m. Through the use of local subdivision, we can conceivably resolve in-

Presented as Paper 85-03896 at the AIAA 23rd Aerospace Sciences Meeting, Reno, NV, Jan. 14-17, 1985; received April 25, 1985; revision received Nov. 6, 1985. Copyright © American Institute of Aeronautics and Astronautics, Inc., 1985. All rights reserved.

*Staff Research Scientist. Member AIAA.
†Program Manager, Member AIAA.
‡Physicist.

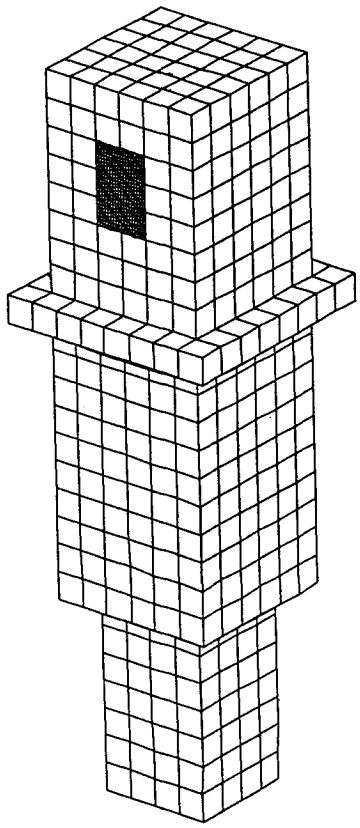

Fig. 1a NASCAP/LEO model of the PIX-II experiment mounted on the Delta booster.

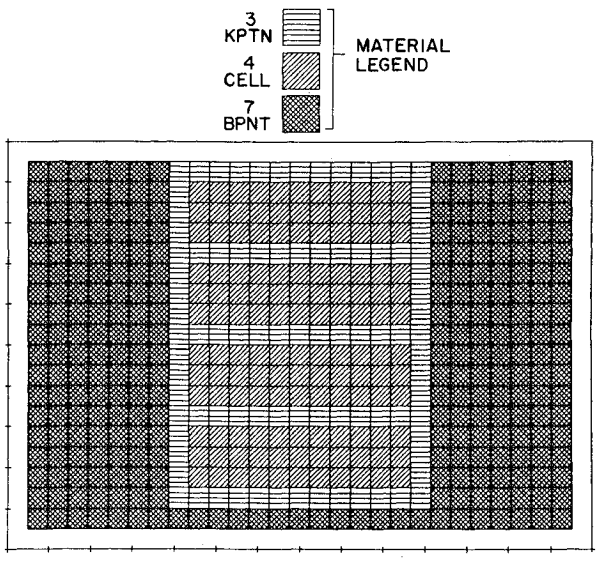

Fig. 1b NASCAP/LEO model of the PIX-II solar panel experiment.

dividual solar cells, but not interconnects. The practice of grouping the interconnects into isolated surface cells has proved inadequate. As this type of surface is of paramount interest, an analytical theory for the solar cell surface potential, consistent with parameters from the main code, is essential.

To construct such a theory, we take advantage of the periodic nature of the solar array surface. Thus the theory will require the distance between interconnects and the fraction of the surface made up by the interconnects. The insulating surfaces will be a few kT negative (with respect to plasma) unless they emit enough low energy secondary electrons to maintain a positive potential. In the latter case, the surface must be nearly neutral ($E_\perp = 0$) to electrons. If it is repelling (secondary electrons escape), it will charge positively; if it is attractive, secondary emission will be suppressed. Thus the theory will predict snapover when the neutral ($E_\perp = 0$) boundary condition leads to the entire insulator's being above its first crossover potential for secondary emission.

Electric Field for Square Wave

Let $2L$ be the solar cell width and $2a$ the effective interconnect width. Consider a potential (Laplacian)

$$V(x,y,0) = \begin{cases} V_0 & -a<x<a \\ 0 & a<x<L \end{cases} \tag{1}$$

$V(x,y,z) = V(-x,y,z) = V(x+26L,y,z)$, defined for $z \geq 0$. We wish to find

$$E_z(L,y,0) = -\frac{\partial V(L,y,z)}{\partial z}\bigg|_{z=0}$$

We may write

$$V(x,y,z) = (V_0 a/L) f(z) + V_0 \sum_{n=1}^{\infty} A_n \cos\frac{n\pi x}{L} e^{-n\pi z/L}$$

$$A_n = \frac{2}{L}\int_0^a \cos\frac{n\pi x}{L}\,dx = \frac{2}{n\pi}\sin\frac{n\pi a}{L} \tag{2}$$

where the term containing $f(z)$ $[f(0)=1]$ describes the dropoff of the mean surface potential, and is determined self-consistently with the electrostatic potential about (and on the scale of) the entire spacecraft.

Now we differentiate to find the electric field at the center of the coverslip.

$$\begin{aligned} E_z(L,y,0) &= (V_0 a/L)\frac{\partial f}{\partial z} \\ &\quad + V_0 \sum_{n=1}^{\infty} \left(\frac{n\pi}{L}\right)\left(\frac{2}{n\pi}\right)(-1)^n \sin\frac{n\pi a}{L} \\ &= E_0 + \frac{2V_0}{L}\sum_{n=1}^{\infty} \sin\frac{2n\pi a}{L} - \sin\frac{(2n-1)\pi a}{L} \\ &= E_0 + \frac{4V_0}{L}\sin\frac{\pi a}{2L} \times \sum_{n=1}^{\infty} \cos\left(2n-\frac{1}{2}\right)\frac{\pi a}{L} \end{aligned} \tag{3}$$

Rewrite the sum as

$$\begin{aligned} \sum_{n=1}^{\infty} \cos\left(2n-\frac{1}{2}\right)\frac{\pi a}{L} &= Re\left\{e^{3\pi i a/2L}\sum_{n=0}^{\infty} e^{2\pi i n a/L}\right\} \\ &= Re\left\{\exp\left(\frac{3\pi i a}{2L}\right)\Big/\left[1-\exp\left(\frac{2\pi i a}{L}\right)\right]\right\} \\ &= \frac{1}{2}\cos\frac{3\pi a}{2L} - \sin\frac{3\pi a}{2L}\sin\frac{2\pi a}{L}\Big/4\sin^2\frac{\pi a}{L} \end{aligned}$$

Finally,

$$E_z(L,y,0) = E_0 - \frac{V_0}{L}\sin\frac{\pi a}{2L} \times \left[\sin\frac{3\pi a}{2L}\sin\frac{2\pi a}{L}\Big/\sin^2\frac{\pi a}{L} - 2\cos\frac{3\pi a}{2L}\right] \tag{4}$$

Application to Solar Array

Consider a solar array surface potential to be periodic in the same sense as above, with potential (in snapped-over condi-

tion) given by

$$V(x,y,0)=\begin{cases} V_I & -b<x<b \\ V_B+(V_I-V_B)\ell n\dfrac{x}{L}\left(2-\dfrac{x}{L}\right) \\ \quad \div \ell n\left[\dfrac{b}{L}\left(2-\dfrac{b}{L}\right)\right] & b<x<2L-b \end{cases} \tag{5}$$

$$V(x,y,z)=V(-x,y,z)=V(x+2L,y,z)$$

(The logarithmic potential is justified because the thin interconnect with $E_\perp=0$ on the insulator is similar to an isolated thin wire.) Here b is the actual interconnect half-width, V_I the interconnect potential, and V_B the potential at the center of the solar cell. We relate to the above square wave potential by defining an effective interconnect fraction

$$\beta=\frac{b}{L}+\int_{b/L}^{1}\frac{\ell n[x(2-x)]}{\ell n[b/L(2-b/L)]}dx$$

$$=\frac{b}{L}+\frac{(2-b/1)[\ell n(2-b/L)-1]-b(b/L)[\ell n(b/L)-1]}{\ell n[(b/L)(2-b/L)]} \tag{6}$$

The mean surface potential is then given by

$$\bar{V}=\beta V_I+(1-\beta)V_B \tag{7}$$

In the limit of zero-energy secondary electrons, the insulating surface will reach equilibrium with $E_z=0$. We apply this condition at $x=L$, to find

$$0=E(L,y,0)=E_0(\bar{V})-\frac{(V_I-V_B)}{L}\gamma(\beta) \tag{8}$$

where [from Eq. (4)]

$$\gamma(\beta)=\sin\frac{\pi}{2}\beta\left[\frac{\sin(3\pi/2)\beta\sin 2\pi\beta}{\sin^2\pi\beta}-\cos\frac{2\pi\beta}{2}\right]$$

Now, assume a linear relationship between the mean electric field and the mean potential. To determine $E_0(\bar{V})$, we write

$$E_0(\bar{V})=\bar{V}/\Delta x \tag{9}$$

where Δx is determined self-consistently using the main code. (Thus Δx is a function of spacecraft geometry, potentials of nearby surfaces, and plasma screening.) We now find [from Eqs. (7), (8), and (9)]

$$\beta V_I+(1-\beta)V_B-\frac{\gamma\Delta x}{L}(V_I-V_B)=0$$

or

$$\frac{V_B}{V_I}=\frac{\gamma\Delta x-L}{\gamma\Delta x+(1-\beta)L} \tag{10}$$

Figure 2 shows values of β, γ, and V_B/V_I for interconnect fractions b/L ranging from 0.01 to 0.10 and three values of $\Delta x/L$. It is apparent that the dependence on $\Delta x/L$, and thus the self-consistency with other geometrical features as solved throught the main code, is critical to an adequate determination of the surface potential.

Dependence on Secondary Electron Crossover

The above solution is valid in a cold plasma only when the potential minimum on the solar cell, V_B, exceeds the first crossover energy, E_I, (typically ~50-100 V) of the insulator's secondary electron yield curve. The two cases remaining are $E_I>V_I$ (including all negative interconnect potentials) and $V_I>E_I>V_B$.

In the "simple" case $E_I>V_I$, the insulator remains near plasma ground (usually a few kT negative), as there is no mechanism to charge it positively. Thus the mean surface potential is the simple area-weighted average of interconnect and conductor potentials.

In the case $V_I>E_I>V_B$, the solar cell is partially snapped over, i.e., there will be enhancement of the interconnect size, but the center of the coverslip remains gounded to the plasma. We approximate the solution by assuming that Eq. (5) is satisfied near the interconnect, up to the point $x=Lx_M$ where the potential drops to E_I. The variable x_M then satisfies

$$E_I=V_B+(V_I-V_B)\frac{\ell n[x_M(2-x_M)]}{\ell n[(b/L)(2-b/L)]}$$

whose solution is

$$x_M=1-\sqrt{1-e^{-\xi}}$$

$$-\xi=\frac{E_I-V_B}{V_I-V_B}\ell n[b/L(2-b/L)]$$

We then find the effective interconnect fraction to be

$$\beta=\frac{b}{L}+\int_{b/L}^{x_M}\frac{\ell n[x(2-x)]}{\ell n[b/L(2-b/L)]}dx$$

$$=\frac{b}{L}+\frac{1}{\ell n[b/L(2-b/L)]}\{x_M(\ell n x_M-1)$$

$$-b/L(\ell n b/L-1)+(2-b/L)[\ell n(2-b/L)-1]$$

$$-(2-x_M)[\ell n(2-x_M)-1]\}$$

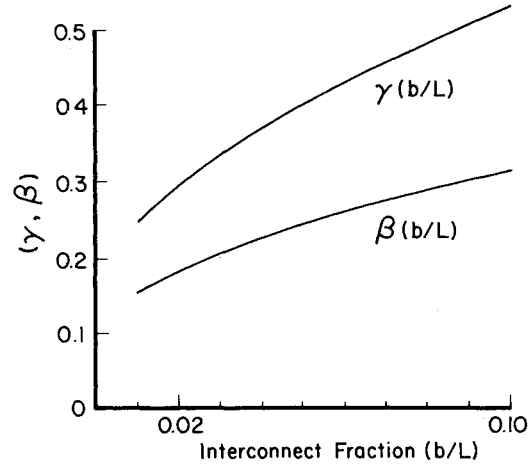

Fig. 2a The effective interconnect fraction (β) and the parameter $\gamma(\beta)$ as a function of actual interconnect fraction.

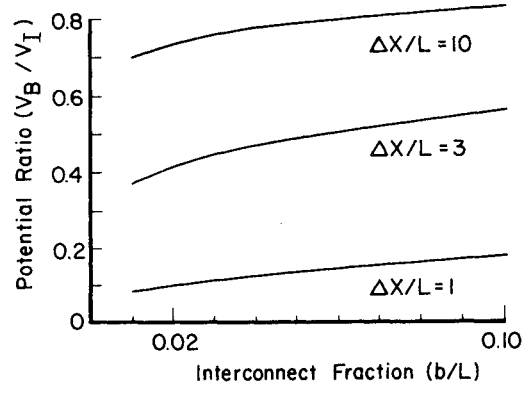

Fig. 2b Ratio of insulator potential (V_B) to interconnect potential (V_I) as a function of actual interconnect fraction for three values of $\Delta x/L$.

Ram and Wake Effects

A satellite in low Earth orbit travels at a speed of about 7500 m/s. As this is faster than the ion thermal speed (about 1400 m/s for an ion mass of 14 amu and a temperature of 0.15 eV), the satellite will leave behind it a very low density "wake." The extent of the wake is determined by the time needed for ions to travel a distance comparable to the spacecraft radius at the ion thermal velocity. In the wake, the electron density, as well as the ion density, is reduced by several orders of magnitude. This is because if this "quasineutral" condition were violated, electrons would be repelled from the region by their own space charge.

The current collected by a probe or other experiment will be strongly affected by its attitude relative to the ram or wake of the spacecraft. In the ram, the dominant ion current will be the ram ions. In the wake, electron current as well as ion current will be greatly reduced. However, the screening of a highly biased probe will also be reduced, which may expand the electrostatic influence of the probe beyond the wake.

In the NASCAP/LEO code, we calculate the ion density in the spacecraft wake using a geometrical shadowing model. The ion density is computed for each cell by integrating the flowing ion distribution function over all velocity directions not obscured by the spacecraft. At the sheath edge, the electron density is taken to be equal to this ion density when computing the thermal flux of electrons entering the sheath. Hence, in regions where the ions are shadowed by the object, the electron density and the electron thermal currents can be dramatically reduced. The second order effect of including the reduced plasma density and thus reduced screening in the potential calculations has not been included. Therefore, the present results tend to underestimate the electron sheath size in the wake.

PIX-II Computational Model

The PIX-II flight experiment consisted of a 2000-cm^2 solar array blanket whose interconnects could be biased either positive or negative up to 1000 V. An electron emitter, mounted on the opposite side of the spacecraft, was used to help control the overall rocket potential. A Langmuir probe was used to obtain an estimate of the environmental parameters.

The NASCAP/LEO computational model (Fig. 1) had 0.25-m resolution over most of the spacecraft, and 0.028-m resolution in the vicinity of the experiment. The solar cells were taken to be 2 cm in size, and to be 6% exposed metal interconnects. The cover slip surfaces were taken to be SiO_2, with maximum secondary emission for normally incident electrons of 4.1 at 410 eV. This composite surface material (cover slips and interconnects) was treated using the analytical model described above. The four solar cell segments were mounted on a kapton substrate, with maximum secondary emission for normally incident electrons to be 2.1 at 150 eV.

The measured plasma density and temperature varied over a wide range during the course of the flight. All calculations presented here assumed an ambient density of 10^4 cm^{-3} and a temperature of 0.15 eV. These conditions correspond to a Debye length of 2.88 cm and a plasma thermal current of 1.04×10^{-4} A/m^2. Thus the electron thermal current to a 2000-cm^2 area would be 0.021 mA. Unless otherwise specified, all calculations were done with the experiment in the ram direction.

For each case the calculation proceeded as follows:

1) Initial potential boundary conditions were specified with the rocket structure at roughly the potential measured in flight, the solar cells at the bias potential, and electric field boundary conditions on the kapton.

2) Two cycles of QUICK-CHARGE-POTENT were run. The QUICK module makes a rough estimate of the currents incident on the surfaces. The CHARGE module estimates the resultant potential change, and the POTENT module calculates the potentials and fields in the space surrounding the spacecraft.

3) The CURRENT module was run to determine the electron current through the sheath surface impinging on the solar array.

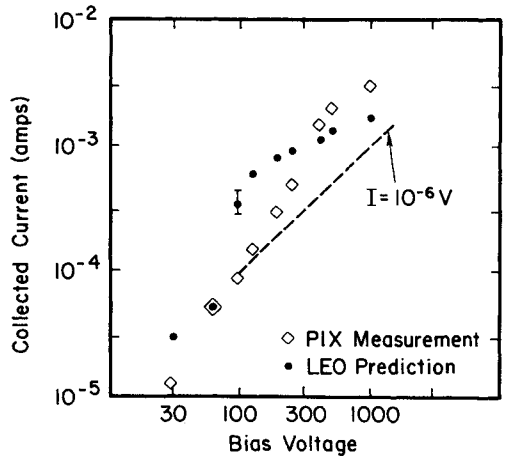

Fig. 3 Flight measurement and NASCAP/LEO prediction of collected electron current for positive bias.

Results

The experimental data and the computational results are shown in Fig. 3 and Table 1. Experimentally, a clear nonlinear increase in the collected current was seen at about 300 volts bias. With no adjustments in the standard NASCAP values for the properties of these materials, NASCAP/LEO predicted a similar increase, but at about 100 V bias. By lowering the peak secondary emission coefficient of the SiO_2 from 4.1 to 2.1, the "snapover" voltage was increased to 200 V. While the above appears to indicate rather poor agreement on the snapover voltage, it should be pointed out that snapover was seen in the laboratory[2] at about 100 V, and at least one other flight experiment curve showed snapover at 200 V.

Figure 4 shows the extent of the electron-collecting sheath for several different bias voltages. Each frame of this figure included potential contours at −0.1 V (surrounding the spacecraft) and +0.1 V (ballooning out from the experiment). The electron current collected is proportional to the area of that part of the sheath not shielded by electrostatic barriers. It is apparent from the figures that below snapover (at 30- and 60-V bias) the sheath remains close to the experiment, while above snapover its area, and therefore the collected current, increases greatly. (Note that the computational space was larger than shown in the figure, so that the boundary conditions did not compress the sheath at the highest voltages.)

Figure 5 shows the change in the character of the surface potential as we proceed through the snapover condition. Below snapover (e.g. at 60-V bias) the solar cell surface is (on average) at about 6% of the bias voltage, while the kapton is

Table 1 Measured and calculated collected currents for positive bias PIX-II experiment

Bias voltage, V	Measured current, mA	Structure potential, V	Calculated current, mA	Snapover
+30	0.1	−0.5	0.03	no
+60	.05	−0.5	0.05	no
+95	.09	−3	0.3	partial
+125	.15	−3	0.6	yes
+190	.3	−4	0.8	yes
+250	.5	−6	0.9	yes
+350	1.5	−10	1.1	yes
+500	2.0	−20	1.3	yes
+1000	3.0	−42	1.6	yes

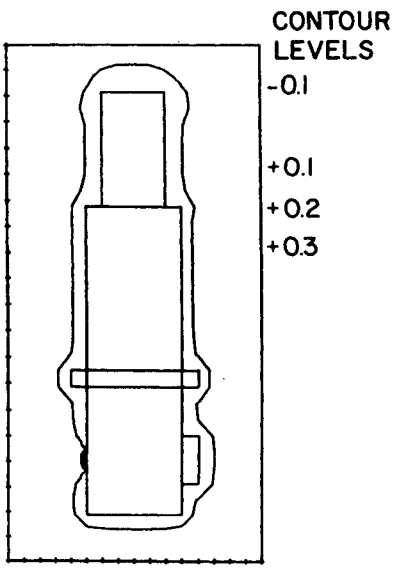

Fig. 4a Potential contours: 30-V bias.

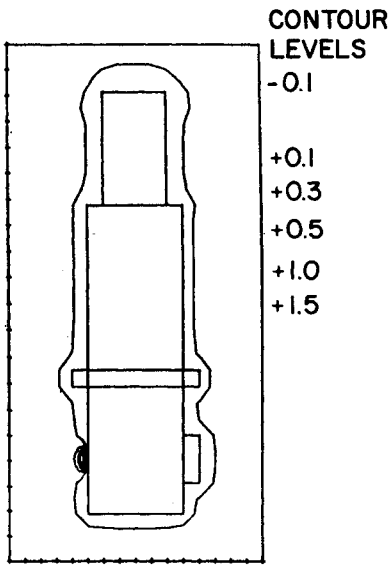

Fig. 4b Potential conoturs: 60-V bias.

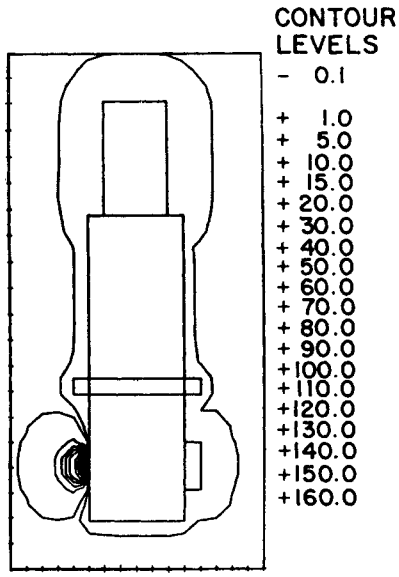

Fig. 4c Potential contours: 95-V bias.

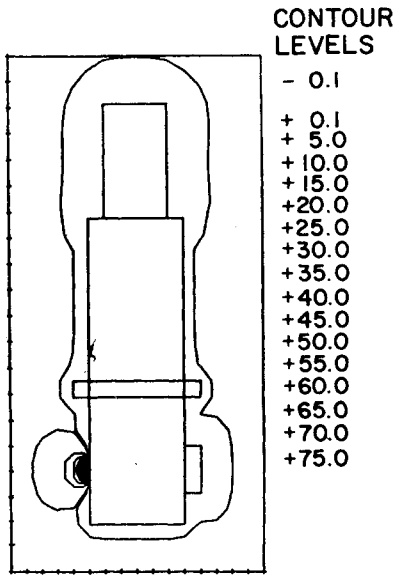

Fig. 4d Potential contours: 190-V bias.

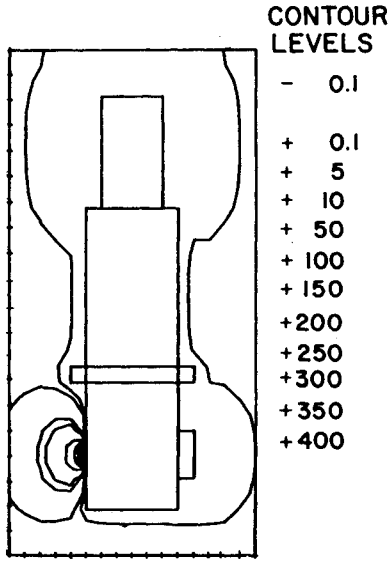

Fig. 4e Potential contours: 500-V bias.

negative. Above snapover (e.g. at 190-V bias) the entire experiment (solar cells and kapton) is (on average) at an appreciable fraction (here about 80%) of the bias voltage. This picture continues until the upper secondary crossover of the kapton is exceeded. Thus at 100-V bias the kapton strips between the solar cell modules can again be seen in the surface potential contours.

It was clearly seen in the experimental measurements that the electron emitter was unable to maintain the rocket structure near plasma ground when the experiment was operated at high bias. To assess this effect, we performed simulations to determine self-consistently the floating potenial of the spacecraft with the experiment biased to 500 V and the emitter off. The floating potential is determined by balance between the ram ion current to the spacecraft cross-sectional area (enhanced by its negative sheath) and the electron current to the experiment. With the experiment in the ram, the floating potential was -73 V, with a collected current of 0.5 mA; with the experiment in the wake, the structure floated at -38 V and the calculated current was 0.4 mA. By contrast, the observed potential was approximately -20 V, at which we calculated 1.3 mA of collected current. Thus we find that the emitter indeed had a substantial effect on the spacecraft floating potential as well as the collected current.

We also performed calculations for the experiment at 135 deg in the spacecraft wake at biases of 60 and 500 V. For the 60-V case, the collected current was reduced to 10^{-10} A from its ram value of 0.05 mA. AT 500-V bias and a potential of -20 V the experiment collected 0.5 mA in the wake, or about half of its ram value. The high-voltage measurements are not so strongly affected by wake effects as the low-voltage results because the much larger high-voltage sheaths typically extend outside the wake region, whereas the small low-voltage sheaths can easily be totally within the spacecraft wake. It is thus very important to know the orientation of the spacecraft for low potentials, and a scatter of experimental results can be expected if the orientation is not constant.

The experimental curve shown in Ref. 7 was apparently taken in the wake. At 60 V bias, the collected current was suppressed by two orders of magnitude and remained suppressed to about 125 V. At 180 V, this curve actually showed more current than Ref. 2, indicating that complete snapover had already occurred. At high voltages the current was about half that shown in Ref. 2, in agreement with our prediction.

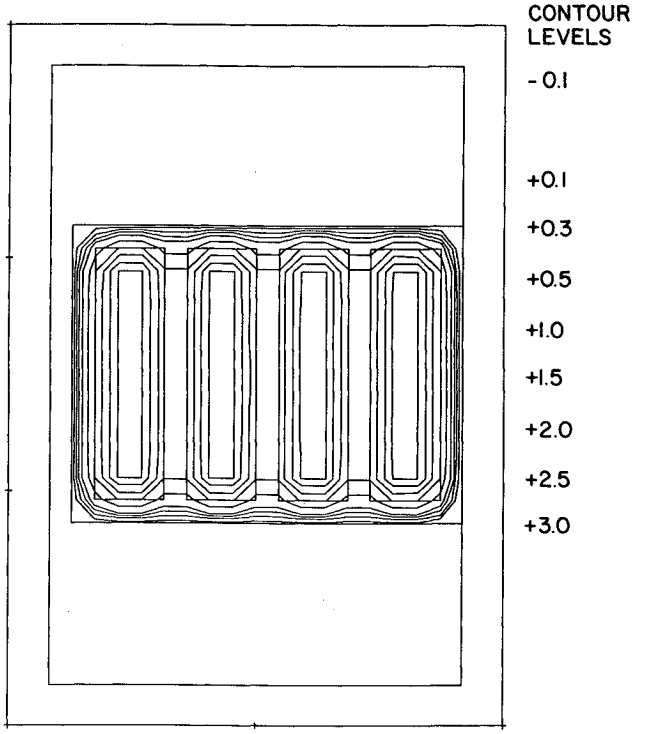

Fig. 5a Potential contours on solar array surface: 60-V bias.

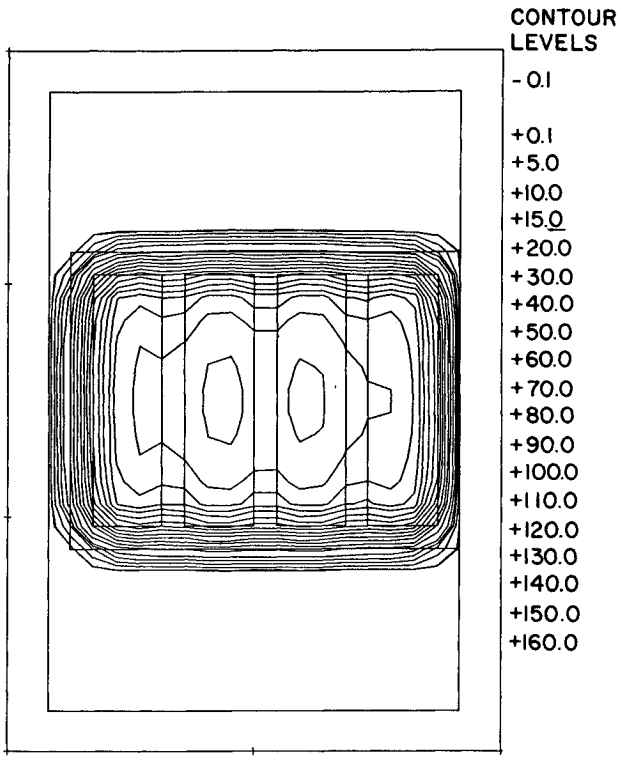

Fig. 5b Potential contours on solar array surface: 190-V bias.

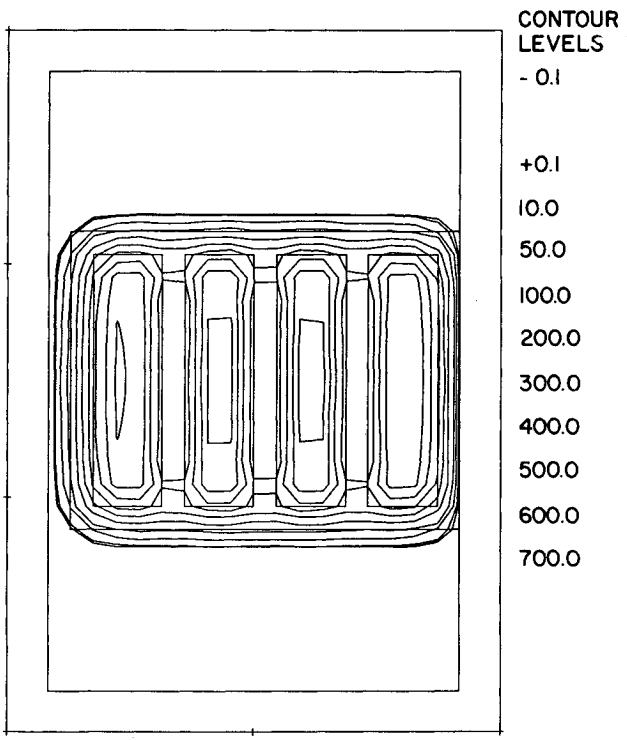

Fig. 5c Potential contours on solar array surface: 1000-V bias.

Discussion

Through the use of an analytical model for a solar array surface, together with local subdivision and other capabilities of the NASCAP/LEO computer code, we have been able to model electron collection by the PIX-II simulated solar array experiment. In comparing the computer results with the flight measurements, it must be remembered that the plasma environment and the spacecraft orientation during flight are very uncertain. Also uncertain are parameters concerning the array surface, such as the first secondary emission crossover and the actual interconnect area.

The NASCAP/LEO code predicted approximately the correct electron current both at high and low positive bias voltage, and showed qualitatively the same snapover phenomenon. At high voltage, more electron current was measured than predicted; this may be attributable to the operation of an electron emitter on the opposite side of the spacecraft, which was only partially successful at its intended purpose of maintaining the spacecraft structure potential near plasma ground. It is easy to imagine that electrons from the emitter were attracted to the large, high potential sheath formed near the experiment at high positive bias.

The least satisfying aspect of the simulation is that snapover was predicted at a much lower voltage than observed. In support of the simulation, laboratory tests of the PIX-II experiment exhibited snapover at bias voltages much nearer the computer prediction. Another explanation might be that the snapover state is, in fact, bistable, and the analytical model outlined here will preferentially choose the high voltage branch. Of course, the difference could also be due to some unknown factor involving the SiO_2 surface and/or the space environment in the vicinity of the spacecraft.

In conclusion, we have demonstrated a computer code capable of modeling electron collection by a biased solar array, taking into account both the fine details of the solar array surface and the electrostatic influence and the wake of the gross spacecraft structure. In developing this model, we have advanced our phenomenological understanding of how solar arrays behave in space, and we have achieved a good start on a quantitative model to be used in the design of advanced solar array power systems.

Acknowledgment

This work was supported by NASA/Lewis Research Center, Cleveland, Ohio, under Contract NAS3-23881.

References

[1]Grier, N.T., Smith, C., and Johnson, L.M., "Plasma Interactions with Solar Arrays at High Voltages," *Spacecraft Charging Technology—1980*, NASA CP-2181, AFGL-TR81-2070, 1981, pp. 922-930.

[2]Grier, N.T., "Plasma Interaction Experiment II: Laboratory and Flight Results," *Spacecraft Environment Interactions Technology Conference,* Colorado Springs, CO, Oct. 4-6, 1983, NASA CP-2359, AFGL-TR-85-0018, pp. 333-348.

[3]Mandell, M.J., Katz, I., and Cooke, D.L., "Potentials on Large Spacecraft in LEO," *IEEE Transactions on Nuclear Science,* NS-29, 6, Dec. 1982, pp. 1584-1587.

[4]Chaky, R.C., Nonnast, J.H., and Enoch, J., "A Numerical Simulation of Plasma-Insulator Interactions in the Spacecraft Environment," *Journal of Applied Physics,* 52, 1981, p. 7092.

[5]Gabriel, S.B., Garner, C.E., and Kitamura, S., "Experimental Measurements of the Plasma Sheath Around Pinhole Defects in a Simulated High-Voltage Solar Array," AIAA Paper 83-0311, Jan. 1983.

[6]Mandell, M.J. and Katz, I., "Potentials in a Plasma Over a Biased Pinhole," *IEEE Transactions on Nuclear Science,* NS-30, 6, Dec. 1983, pp 4307-4310.

[7]Roche, J.C. and Mandell, M.J., "NASCAP Simulation of the PIX-II Experiments," *Spacecraft Environment Interactions Technology Conference,* Colorado Springs, CO, Oct. 4-6, 1983, NAS CP-2359, AFGL-TR-85-0018, pp. 258-366.

From the AIAA Progress in Astronautics and Aeronautics Series

THERMOPHYSICS OF ATMOSPHERIC ENTRY—v. 82

Edited by T.E. Horton, The University of Mississippi

Thermophysics denotes a blend of the classical sciences of heat transfer, fluid mechanics, materials, and electromagnetic theory with the microphysical sciences of solid state, physical optics, and atomic and molecular dynamics. All of these sciences are involved and interconnected in the problem of entry into a planetary atmosphere at spaceflight speeds. At such high speeds, the adjacent atmospheric gas is not only compressed and heated to very high temperatures, but stongly reactive, highly radiative, and electronically conductive as well. At the same time, as a consequence of the intense surface heating, the temperature of the material of the entry vehicle is raised to a degree such that material ablation and chemical reaction become prominent. This volume deals with all of these processes, as they are viewed by the research and engineering community today, not only at the detailed physical and chemical level, but also at the system engineering and design level, for spacecraft intended for entry into the atmosphere of the earth and those of other planets. The twenty-two papers in this volume represent some of the most important recent advances in this field, contributed by highly qualified research scientists and engineers with intimate knowlege of current problems.

Published in 1982, 521 pp., 6×9, illus., $35.00 Mem., $55.00 List

TO ORDER WRITE: Publications Dept., AIAA, 1633 Broadway, New York, N.Y. 10019